Progress In Electromagnetics Research C, Vol. 26, 43–57, 2012

COMPACT METAL MOUNTABLE UHF RFID TAG ON A BARIUM TITANATE BASED SUBSTRATE

T. Bjorninen[1,*], A. A. Babar[1], L. Ukkonen[1], L. Sydanheimo[1], A. Z. Elsherbeni[2], and J. Kallioinen[3]

[1]Department of Electronics, Tampere University of Technology, Kalliokatu 2, FI-26100 Rauma, Finland

[2]Department of Electrical Engineering, University of Mississippi, MS 38677-1848, USA

[3]Sachtleben Pigments Oy, Titaanitie, FI-28840 Pori, Finland

Abstract—The development of a compact metal mountable Radio-Frequency IDentification (RFID) tag antenna on a ceramic substrate based on Barium Titanate is presented. The performance limitations and design trade-offs of metal mountable RFID tag antennas are reviewed and the favorable features of a high-permittivity antenna substrate for the development of antennas for metal mountable RFID tags are discussed. The simulation-based tag antenna design process is outlined and the measured read range of the developed metal mountable tag on conductive platforms of various sizes is presented.

1. INTRODUCTION

Versatile and energy efficient passive radio-frequency identification (RFID) technology [1] is a strong candidate to replace some of the present automatic identification systems, based on the visual line of sight connection, biometric identification, and tracking assets with active transmitters. The advantages of RFID in asset tracking and supply chain management [2] are already widely recognized, but there are still unresolved issues related to the design of RFID tags for the identification of objects containing or consisting of materials with adverse effect on the operation of antennas. A pronounced example of such materials are metals. Nevertheless, metallic objects are encountered continually in applications of RFID and thus it

Received 2 November 2011, Accepted 25 November 2011, Scheduled 9 December 2011

* Corresponding author: Toni Björninen (toni.bjorninen@tut.fi).

is important to explore tag antenna design approaches further to guarantee reliable identification of these objects as well.

In RFID applications seamless integration of the tags with the objects is a common constraint for the tag antenna design. In identification of metallic objects this means that the tag antenna needs to be parallel to a conducting surface in order to minimize the additional space occupied by the tag. However, placing a transmitting antenna parallel to a conducting surface induces an image current with opposite phase in the conducting surface. With the antenna distance much less than a quarter wavelength from the surface, the electromagnetic fields radiated by the image current and the antenna sum up with approximately 180° phase difference and cancel each other largely. Consequently the antenna radiation radiation efficiency is low. Further, the proximity of the metal surface (even a small one compared with the antenna) can greatly affect the antenna impedance and radiation pattern [3, 4] compared with the properties of an isolated antenna. By the reciprocity theorem, the same observations hold for receiving antennas [3] and thereby for RFID tags in particular. In practice, neglecting the electromagnetic interaction between the tag antenna and the conducting surface, while using standard general purpose tags to label conductive objects, compromises the reliability of the identification [5–7].

One of the key-issues in the design of metal mountable tags is the trade-off between the tag antenna size and its performance on metal. For example, 3.1-meter read range is achieved with a high impedance unit cell based tag with the size of $60 \times 20 \times 1.5\,\mathrm{mm}^3$ [8], 3.4-meter read range is reported for a meandered patch-type tag antenna with the size of $83 \times 35 \times 0.8\,\mathrm{mm}^3$ [9], a T-shaped slot antenna with size of $120 \times 35 \times 5.05\,\mathrm{mm}^3$ has 14-meter read range [10], and 25-meter read range is obtained with a rectangular patch tag with an inductive feed network and size of $131 \times 68 \times 3.3\,\mathrm{mm}^3$ [11]. An absolute comparison between these tags may not be justified, since the read ranges are reported on different conducting platforms and different tag ICs have been used. However, with these examples, the fundamental trade-off between the tag antenna size and the tag read range is exemplified.

As opposed to read range driven antenna design for metal mountable RFID tags, it is worth noticing that long read range of several meters is not always required, and in fact some high-performance metal mountable tags may already be larger in size than small metallic objects encountered in item level RFID. Moreover, compared with patch antennas which are widely used in metal mountable RFID tags, the inherently ball-like radiation pattern of dipoles and slots in the proximity of metal [3] could actually provide

improved spatial coverage, given that other issues due to the metal proximity were sufficiently addressed. Motivated by these observations, we have studied an alternative antenna design approach for metal mountable RFID tags, focusing primarily on tag size constraints rather than aiming for very long read range. The compact size of the developed tag antenna reported in this article has been achieved with the help of high-permittivity ceramic tag antenna substrate based on Barium Titanate ($BaTiO_3$). Due to its small size, the developed tag is suitable especially for identification of small metallic objects, but it operates well on larger conductive platforms as well.

2. THEORETICAL BACKGROUND AND TAG PERFORMANCE CONSIDERATIONS

Passive RFID tags consist of an antenna and an integrated circuit (IC). Evidently, efficient power transfer from the tag antenna to the tag IC is a crucial design aspect for passive tags, since they are remotely powered by the reader. For the purpose of tag antenna design, the antenna-IC power transfer efficiency can be analyzed based on a series equivalent circuit where these two components are joined with a transmission line of a negligible electrical length. In this setting, the tag antenna acts as a generator with an internal impedance Z_a and source voltage amplitude V_a, and delivers power to the tag IC with input impedance Z_{ic}. Letting V_{ic} and I_{ic} be the tag IC voltage and current amplitudes, respectively, the standard complex phasor calculus provides the time-average power delivered to the tag IC:

$$P_{ic} = \frac{1}{2}\mathrm{Re}\left(\tilde{V}_{ic}\tilde{I}_{ic}^{*}\right) = \frac{1}{2}\mathrm{Re}\left(\frac{Z_{ic}}{Z_a + Z_{ic}}\tilde{V}_a\left(\frac{\tilde{V}_a}{Z_a + Z_{ic}}\right)^{*}\right) = \frac{1}{2}\frac{\mathrm{Re}\left(Z_{ic}\right)}{\left|Z_a + Z_{ic}\right|^2}V_a^2. \quad (1)$$

Here $\tilde{(\cdot)}$ identifies the complex voltage and current phasors and $(\cdot)^*$ denotes the complex conjugate. As it is well-known that P_{ic} is maximized with $Z_a = Z_{ic}^*$, the antenna-IC power transfer efficiency is

$$\tau = \frac{P_{ic}}{P_{ic}\big|_{Z_a = Z_{ic}^*}} = \frac{4\mathrm{Re}\left(Z_a\right)\mathrm{Re}\left(Z_{ic}\right)}{\left|Z_a + Z_{ic}\right|^2}. \quad (2)$$

In free space the read range of a passive UHF RFID tag is typically limited by the reader-to-tag link, since the power required for activating the tag IC is orders of magnitude larger than the weakest backscattered tag signal that can be detected at the reader [17]. Although the free space channel model [18] may not be adequate in real application environments [19] or in the presence of strong tag-to-tag coupling [20], it is well-suited for tag antenna design verification

in controlled environment. Moreover, in applications such as the one considered in this article, with relatively short tag read range, the effect of the multipath propagation is limited [19].

In free space with the transmitted power is limited by the regulated isotropically radiated power EIRP [1, 12], the power captured by the tag antenna and delivered to the tag IC equals to

$$P_{ic} = \tau \chi_{pol} e_{r,\,tag} D_{\text{tag}} \left(\frac{\lambda}{4\pi d} \right)^2 \text{EIRP}, \tag{3}$$

where χ_{pol} is the polarization mismatch factor between the tag and transmitter antenna, $e_{r,\,tag}$ and D_{tag} are the tag antenna radiation efficiency and directivity, respectively, and d is the separation between the reader antenna and the tag. Thus, the performance of reader-to-tag link is determined by the realized tag antenna gain defined as $G_{r,\,\text{tag}} = \tau e_{r,\,\text{tag}} D_{\text{tag}}$. An estimate for the tag read range based on (3) is

$$d_{\text{tag}} = \frac{\lambda}{4\pi} \sqrt{\frac{\chi_{pol} G_{r,\,\text{tag}} \text{EIRP}}{P_{ic,0}}}, \tag{4}$$

where $P_{ic,0}$ is the wake-up power of the tag IC.

As the wake-up powers of tag ICs are reaching -18 dBm and below [13–16], very high realized tag antenna gain is no longer an absolute requirement for achieving one to three meters of read range. Consequently, as one of the issues with small antennas is the difficulty of achieving high radiation efficiency [21], for RFID applications where aggressive tag miniaturization is required, trading-off a portion of the radiation efficiency for size-reduction purposes may be a feasible design approach. This is illustrated in Fig. 1, where the tag read range calculated with (4) is presented as a function of the tag IC wake-up power for various low values of the tag antenna radiation efficiency.

The reason why Fig. 1 has been created considering a rather low directivity ($D_{\text{tag}} = 1.8$ dBi) compared with the values reported for metal mountable tags [8–11], is that the aim of the present work is to develop a tag suitable for identification of small metallic objects. In this case, the potential improvement in tag antenna directivity due to an electrically large metal plate backing the tag antenna cannot be expected. Therefore, the smallest possible metal plate that the antenna can fit on should be considered in the design.

The important observation from Fig. 1 is that with tag IC wake-up powers of -18 dBm and below, longer than one meter read range is still achievable, provided that the tag antenna is reasonably well matched ($\tau \geq 0.75$).

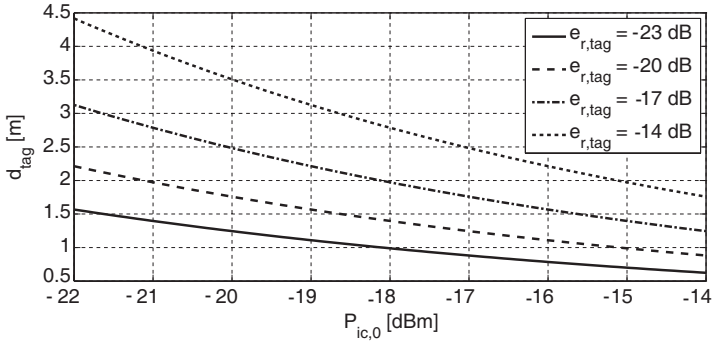

Figure 1. Tag read range as a function the tag IC wake-up power at 915 MHz for various low values of the tag antenna radiation efficiency with $D_{\text{tag}} = 1.8\,\text{dBi}$, $\tau = 0.75$, $\chi_{pol} = 1$ and EIRP $= 4\,\text{W}$.

3. TAG ANTENNA DESIGN

The tag antenna reported in this article is designed for Higgs-3 EPC Generation 2 Class 1 compatible UHF RFID IC from Alien Technology [13] with the reported wake-up power of $-18\,\text{dBm}$. The IC is provided by the manufacturer in a strap fixture which is readily mounted on the prototype tag antenna for testing purposes. For impedance matching analysis, we have chosen to model the tag IC based on the measured tag IC input impedance reported in [22]. The measured data includes the strap parasitics and is the IC input impedance at the wake-up power of the IC. In order to obtain a more flexible model for design purposes, polynomial fits weighted with the inverse of the reported measurement uncertainty were created. The measured data points and the associated polynomial fits are shown in Fig. 2.

Due to its high permittivity, $BaTiO_3$ as an antenna substrate could provide a lower antenna self-resonance frequency compared with standard microwave circuit board materials [21]. In addition, for the development antennas for metal mountable tags, a favorable feature of a high-permittivity tag antenna substrate is that it increases the electrical separation of the antenna from the metal surface by a factor of $\sqrt{\epsilon_r}$ compared to the physical distance. This helps to mitigate the adverse effects of the image current. The antenna substrate we use is a ceramic disk consisting of 90% of $BaTiO_3$ and 10% of Aluminium Oxide. The latter compound is included to provide sufficiently durable structural properties for testing. The diameter and thickness of the disk are 27.5 mm and 2.75 mm, respectively, which means that at the

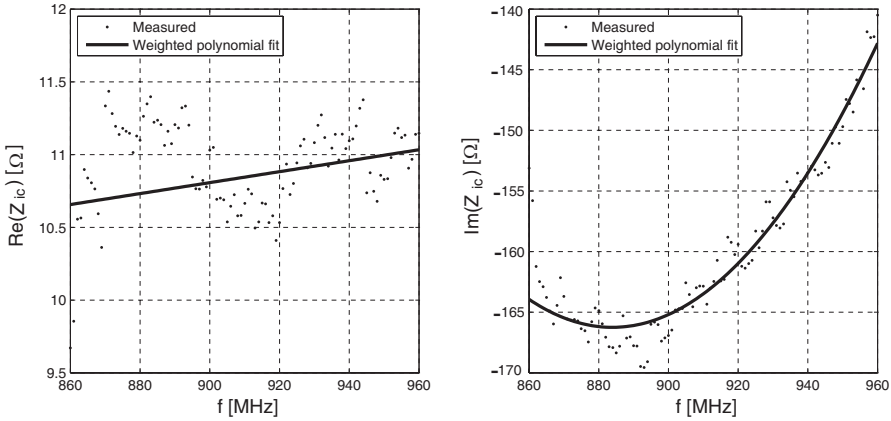

Figure 2. Tag IC impedance model used in the tag simulations.

design frequency of 915 MHz, the tag antenna foot-print size is less than 0.09λ.

As discussed earlier, the image current in the metal surface beneath the tag is a major factor to consider in the design of antennas for metal mountable tags. To better understand this effect in our design, an initial study with a dipole antenna and a slot antenna placed on the ceramic disk backed by a copper plate with size of $30 \times 30\,\mathrm{mm}^2$ was conducted using ANSYS HFSS fullwave electromagnetic simulator based on finite element method [23]. As $BaTiO_3$ may have significant dielectric losses [24] and the added Aluminium Oxide is expected to decrease the dielectric constant of the disk compared with pure $BaTiO_3$, values $\epsilon_r = 39$ and $\tan\delta = 0.02$ were used to model its dielectric properties. This estimate was also justified indirectly by comparing simulation and measurement results, as explained below.

The amplitude of the simulated current induced in the copper plate in case of a dipole and slot antenna is shown in Fig. 3. Shapes of these antennas were chosen in accordance with small antenna design principles to occupy the available space with conductor as much as possible, while avoiding current cancellation [25]. As seen from Fig. 3, the peak current in the copper plate due to the slot antenna is much lower than that of the dipole, while the region with the current amplitude less than 55 S/m is similar for both antennas. Based on this comparison, the slot configuration was chosen for further development.

Further simulations with the slot antenna studied in Fig. 3 were done to investigate how its fundamental resonance frequency is affected by the substrate permittivity. Anticipating that the prototype

antenna is fabricated with the standard milling method on an FR-4 board, the board with thickness of 0.16 mm was included in the simulation model in between the ceramic disk and the antenna as shown in Fig. 4. The FR-4 board was modeled with the dielectric properties: $\epsilon_r = 4.4$ and $\tan\delta = 0.02$. Although, ideally the antenna would be fabricated directly on the ceramic substrate, the present approach with the thin FR-4 board to facilitate testing is acceptable to demonstrate the proposed tag concept. As a future research topic, potential performance improvement by depositing the antenna conductor directly on the ceramic substrate using printable

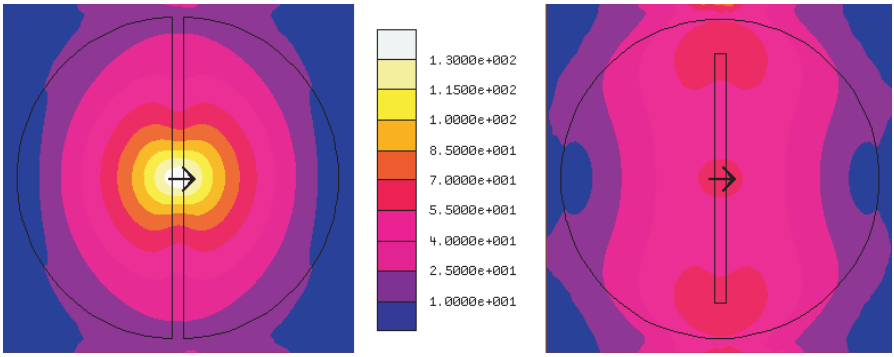

Figure 3. Current amplitude in a copper plate beneath dipole (on the left) and slot (on the right) antennas, both accepting 100 mW power. The impressed source current is indicated with the black arrows. Black lines show the antenna outlines.

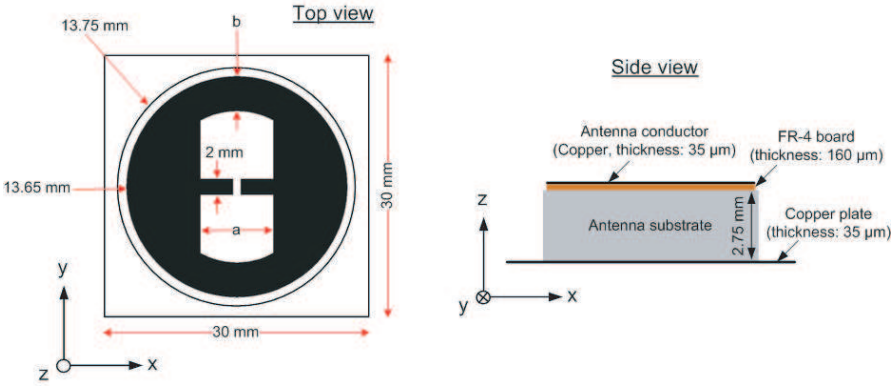

Figure 4. Size and shape of the prototype tag antenna.

Table 1. Fundamental resonance frequency of the slot antenna shown in Fig. 3 versus the dielectric constant of the substrate disk.

ϵ_r	15	20	25	30	35
f_{res} [GHz]	1.477	1.325	1.225	1.15	1.093
ϵ_r	40	45	50	55	60
f_{res} [GHz]	1.049	1.013	0.982	0.957	0.935

electronics [26] could be addressed.

The obtained simulation results, listed in Table 1, clearly indicate how the fundamental resonance frequency of the antenna decreases, while its substrate dielectric constant increases. This justifies the proposed size-reduction aspect of the high-permittivity tag antenna substrate in the considered application. In addition, a slot antenna (complementary dipole) is an advantageous choice from the point of view of impedance matching, since according Babinet's principle [3] it has an inherently inductive input impedance below the fundamental resonance frequency. This means that it can be conjugate matched with capacitive tag IC impedance (see Fig. 2) already below the fundamental resonance frequency. In contrast, a short dipole with inherently capacitive input impedance, would require an additional matching network to provide the conjugate impedance matching.

Following the feasibility considerations discussed above, six different test tag antennas based on the geometry shown in Fig. 4 were designed for maximal power transfer efficiency (τ) given in (2) at 915 MHz, assuming dielectric constants $\epsilon_r = 37, 38, \ldots, 42$ and loss tangent $\tan\delta = 0.02$ for the ceramic substrate. For each test tag antenna, the input impedance was tuned by varying the parameters a and b to maximize τ.

Wireless tag measurements discussed in more detail in the next Section, showed that the initial guess $\epsilon_r = 39$ resulted in close agreement between the simulated and measured optimal operation frequency of the tag. As the tag IC impedance model has been proven to be reliable earlier in simulation-based tag design [11], the discrepancies between the simulation and measurement results observed with the other test tags were contributed mainly on incorrect dielectric parameters to model the tag antenna substrate. Thus, the test tag antenna designed with parameters $\epsilon_r = 39$ and $\tan\delta = 0.02$ was considered as the final prototype and further experimental characterization was conducted with this tag antenna only.

Referring to Fig. 4, the values of the dimensional parameters of the prototype tag antenna geometry are $a = 9$ mm, and $b = 4.3$ mm.

The simulated impedance matching characteristics of the prototype tag antenna are presented in Fig. 5. Its directivity patterns (on a $30\times30\,\text{mm}^3$ copper plate) are shown in Fig. 6, and the relevant antenna design data at 915 MHz is summarized in Table 2.

As seen from the simulation results in Fig. 5, the power transfer efficiency calculated with (2) is maximized around 915 MHz. The simulated directivity in Fig. 6 indicate that on the copper plate (with size of only $30 \times 30\,\text{mm}^2$), the radiation pattern of the tag antenna is omnidirectional with peak value of 2.6 dBi in the direction of the

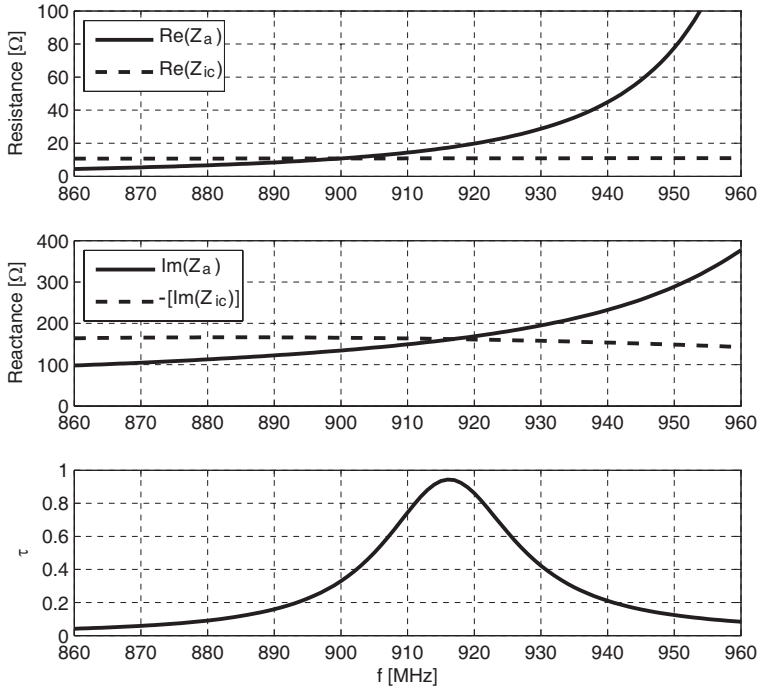

Figure 5. Simulated tag antenna impedance, the conjugate of the tag IC impedance, and the resulting power transfer efficiency.

Table 2. Antenna design data at 915 MHz.

$Z_a\,[\Omega]$	$Z_{ic}\,[\Omega]$	τ	D_{tag} [dBi]
$16.8 + j158$	$11 - j162$	0.93	2.6
$e_{r,\,\text{tag}}$ [dB]	G_{tag} [dBi]	$G_{r,\,\text{tag}}$ [dBi]	d_{tag} [m]
-19.5	-16.8	-17.2	1.8

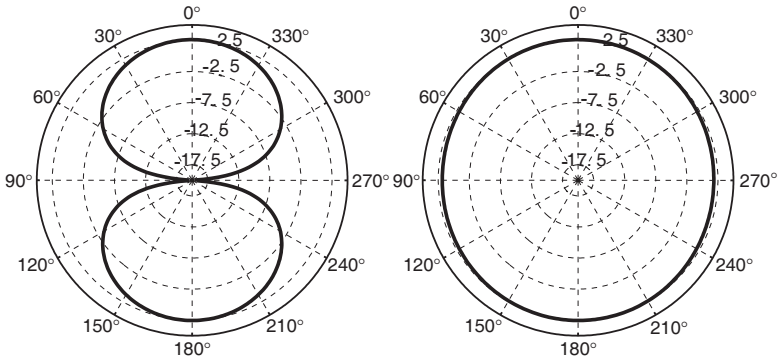

Figure 6. Simulated tag antenna directivity [dBi] at 915 MHz in xz-plane (on the left) and in yz-plane (on the right) in Fig. 4.

positive z-axis as shown in Fig. 4. As discussed earlier, it is important to take this into account in the simulation-based design and optimize the antenna considering the smallest possible metal plate, since a larger plate potentially increases the antenna directivity. This could lead to overestimation of the tag read range. Overall, the simulations predict a read range of 1.8 m, despite the seemingly low radiation efficiency of −19.5 dB. However, this prediction is in agreement with the initial considerations presented in Section 2 and is explained by the good antenna-IC power transfer efficiency and wake-up power of the tag IC.

4. EXPERIMENTAL RESULTS AND DISCUSSION

Measuring the tag read range directly by taking the tag farther away from the reader antenna until its response stops has the disadvantage that the reflections from the surroundings may affect the outcome. Conducting this measurement in an anechoic chamber avoids this problem, but since the anechoic chambers are often limited in size, an alternative method based on the ramping of the transmitted power is advantageous. In this way, also higher repeatability and accuracy are achieved, since neither the tag nor the reader antenna needs to be moved during the measurement.

To obtain the read range and the realized gain of the tag antenna using the power ramping method, EPC Generation 2 query command (to which the tag replies with its identification code) was sent to the tag under test, while illuminating it with a decreasing carrier power density. The measured quantity was the threshold power (P_{th}), the minimum transmitted carrier power, which enables a valid response

from the tag. The threshold power measurement was conducted in a compact anechoic chamber with Voyantic Tagformance Lite measurement device [27], which is a measurement unit for RFID tag performance characterization. It allows power ramping at a defined frequency and thereby the threshold power analysis.

The threshold power measurement was conducted from 860 MHz to 960 MHz with 0.5 MHz steps, while the transmitted power ranged from 0 to 28 dBm with 0.1 dB steps. Using the calibration procedure of the device, the wireless measurement channel was characterized in terms of the measured link loss factor (L_{iso}) from the generator's output port to the input port of an equivalent isotropic antenna placed at the tag's location. During the measurement, the tag under test was carefully aligned to match with the polarization of the linear transmitting antenna to avoid additional link loss due to polarization mismatch. In this way, the measured P_{th} can be mapped to its theoretical value in free space for comparison with the simulations. The free space read range based on the measured P_{th} and L_{iso} is given by

$$d_{\text{tag}} = \frac{\lambda}{4\pi}\sqrt{\frac{\text{EIRP}}{L_{iso}P_{th}}}. \tag{5}$$

The measured results, including the raw measurement data, as well as the free space read range calculated with (5) following the US power regulation EIRP = 4 W, are shown in Fig. 7. In order to obtain a more holistic characterization of the performance of the prototype tag, the measurement was repeated with the tag mounted on four square-shaped copper plates with side lengths shown in the figure legend. For the two of the largest plate sizes, the tag under test had to be placed slightly off from the main beam of the transmitting antenna, which resulted in slightly increased link loss. However, this is accounted for in the read range calculation and does not affect the outcome of the measurement.

As seen from the measured results in Fig. 7 the performance of the designed tag actually improves significantly with the increasing size of the conductive platform. This justifies the prosed design approach for compact metal mountable tags, where the tag antenna is co-designed with the smallest expected conductive platform.

At 915 MHz, the simulated and measured read ranges shown in Table 2 and Fig. 7, respectively, with the tag under test mounted on a 3 cm copper plate are 1.8 m and 1.2 m, respectively. The discrepancy between these values can be attributed to the uncertainty in the loss tangent value ($\tan\delta = 0.02$) used to model the dielectric losses in the ceramic substrate. In practice, this value may be higher. Nevertheless, the measurement results indicate that the simulation

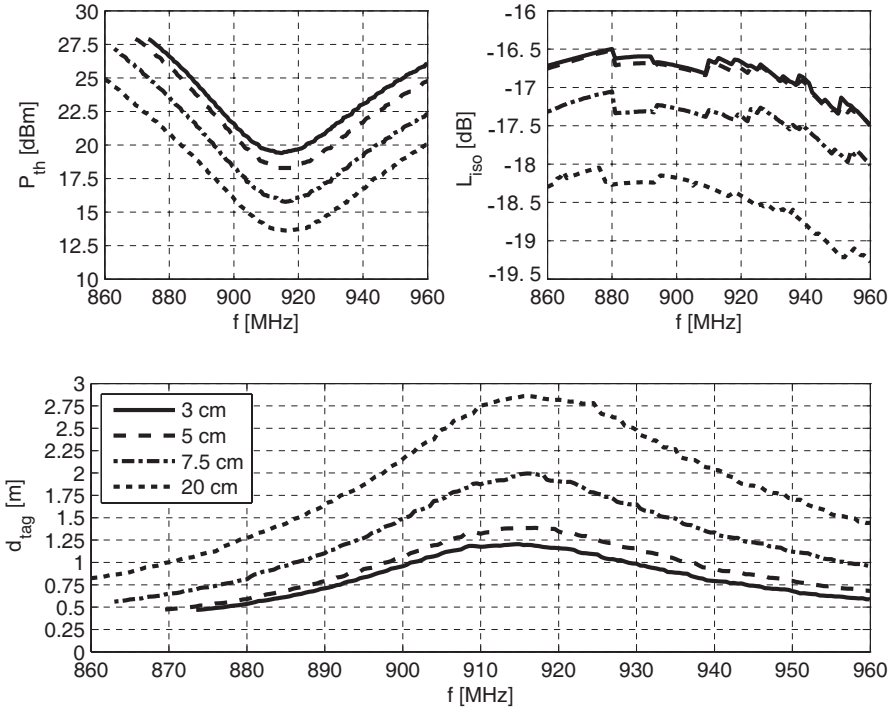

Figure 7. Measured tag read range in the direction of positive z-axis in Fig. 4.

with the dielectric constant of $\epsilon_r = 39$ provides good agreement between the simulated and measured optimum operation frequency. In addition, the measurement results verify the feasibility of the proposed compact metal mountable tag concept, where the tag size is reduced to less than 0.09λ with the help of a high-permittivity tag antenna substrate, while maintaining sufficient tag performance for item level RFID.

5. CONCLUSIONS

A compact metal mountable RFID tag with a ceramic Barium Titanate based antenna substrate was proposed for identification of small metallic objects. Performance limitations and design trade-offs of metal mountable tags were reviewed and the simulation based design of the proposed tag was outlined. Both, the presented simulations and experimental work verified the feasibility of the proposed compact

metal-mountable tag based on a high-permittivity antenna substrate.

As a future research topic, we will develop a similar tag on a flexible high-permittivity substrate for identification of small metallic objects with curved surface, and investigate the potential performance improvement by depositing the antenna conductor directly on the substrate using printable electronics.

ACKNOWLEDGMENT

This research work was funded by the Finnish Funding Agency for Technology and Innovation (TEKES), Academy of Finland, Centennial Foundation of Finnish Technology Industries, Tampere Doctoral Programme in Information Science and Engineering (TISE), HPY Research Foundation, and Ulla Tuominen Foundation.

REFERENCES

1. Dobkin, D., *The RF in RFID: Passive UHF RFID in Practice*, Newnes-Elsevier Inc., Burlington, MA, USA, 2008.
2. Michael, K. and J. McCathie, "The pros and cons of RFID in supply chain management," *International Conference on Mobile Business*, 623–629, Sydney, Australia, July 11–13, 2005.
3. Elliot, R. S., *Antenna Theory and Design*, An IEEE Classical Reissue, John Wiley & Sons, Inc., Hoboken, New Jersey, 2003.
4. Raumonen, P., L. Sydanheimo, L. Ukkonen, M. Keskilammi, and M. Kivikoski, "Folded dipole antenna near metal plate," *IEEE Antennas and Propagation Society International Symposium*, 848–851, Columbus, Ohio, USA, June 22–27, 2003.
5. Foster, P. R. and R. A. Burberry, "Antenna problems in RFID systems," *IEE Colloquium on RFID Technology*, 3/1–3/5, London, UK, October 25, 1999.
6. Griffin, J. D., G. D. Durgin, A. Haldi, and B. Kippelen, "RF tag antenna performance on various materials using radio link budgets," *IEEE Antennas Wireless Propag. Lett.*, Vol. 5, No. 1, 247–250, 2006.
7. Aroor, S. R. and D. D. Deavours, "Evaluation of the state of passive UHF RFID: An experimental approach," *IEEE Syst. J.*, Vol. 1, No. 2, 168–176, 2007.
8. Chen, S.-L. and K.-H. Lin, "A slim RFID tag antenna design for metallic object applications," *IEEE Antennas Wireless Propag. Lett.*, Vol. 7, No. 1, 729–732, 2008.

9. Chen, H.-D. and Y.-H. Tsao, "Low-profile meandered patch antennas for RFID tags mountable on metallic objects," *IEEE Antennas Wireless Propag. Lett.*, Vol. 9, No. 1, 118–121, 2010.
10. Park, S. Y., J. N. Lee, and J. K. Park, "Design of UHF radio frequency identification metal tag antenna using T-shaped slot," *Microwave and Optical Technology Letters*, Vol. 53, No. 10, 2011.
11. Bjorninen, T., K. Espejo Delzo, L. Ukkonen, A. Z. Elsherbeni, and L. Sydanheimo, "Long range metal mountable tag antenna for passive UHF RFID systems," *IEEE RFID Technologies and Applications Conference*, 194–198, Sitges, Spain, Sept. 15–16, 2011.
12. EPCglobal Frequency Regulations, UHF, http://www.gs1.org/epcglobal/implementation.
13. Alien Technology, Morgan Hill, CA, USA, http://www.alientechnology.com.
14. Impinj Inc., Seattle, WA, USA, http://www.impinj.com/.
15. Curty, J.-P., N. Joehl, C. Dehollain, and M. J. Declercq, "Remotely powered addressable UHF RFID integrated system," *IEEE J. Solid-State Circuits*, Vol. 40, No. 11, 2193–2202, 2005.
16. Mandal, S. and R. Sarpeshkar, "Low-power CMOS rectifier design for RFID applications," *IEEE Trans. Circuits Syst. I, Reg. Papers*, Vol. 54, No. 6, 1177–1188, 2007.
17. Nikitin, P. V. and K. V. S. Rao, "Antennas and propagation in UHF RFID systems," *IEEE International Conference on RFID*, 277–288, Las Vegas, NV, USA, Apr. 16–17, 2008.
18. Friis, H. T., "A note on a simple transmission formula," *Proc. IRE*, Vol. 34, No. 5, 254–256, 1946.
19. Marrocco, G., E. Di Giampaolo, and R. Aliberti, "Estimation of UHF RFID reading regions in real environments," *IEEE Antennas Propag. Mag.*, Vol. 51, No. 6, 44–57, 2009.
20. Yojima, H., Y. Tanaka, Y. Umeda, O. Takyu, M. Nakayama, and K. Kodama, "Analysis of read range for UHF passive RFID tags in close proximity with dynamic impedance measurement of Tag ICs," *IEEE Radio and Wireless Symposium*, 110–113, Phoenix, AZ, USA, Jan. 16–19, 2011.
21. Hansen, R. C., *Electrically Small, Superdirective, and Superconducting Antennas*, John Wiley & Sons, Inc., Hoboken, New Jersey, 2006.
22. Bjorninen, T., M. Lauri, L. Ukkonen, R. Ritala, A. Z. Elsherbeni, and L. Sydanheimo, "Wireless measurement of RFID IC impedance," *IEEE Trans. Intrum. Meas.*, Vol. 60, No. 9, 3194–

3206, 2011.

23. ANSYS Inc., Canonsburg, PA, USA, http://www.ansys.com/.
24. Middleton, W. M., *Reference Data for Engineers: Radio, Electronics, Computer, and Communications*, Newnes-Butterworth-Heinemann, Woburn, MA, USA, 2002.
25. Best, S. R. and J. D. Morrow, "On the significance of current vector alignment in establishing the resonant frequency of small space-filling wire antennas," *IEEE Antennas Wireless Propag. Lett.*, Vol. 2, 201–204, 2003.
26. Subramanian, V., J. M. J. Frechet, P. C. Chang, D. C. Huang, J. B. Lee, S. E. Molesa, A. R. Murphy, D. R. Redinger, and S. K. Volkman, "Progress toward development of all-printed RFID Tags: Materials, processes, and devices," *Proc. IEEE*, Vol. 93, No. 7, 1330–1338, 2005.
27. Voyantic Ltd., Espoo, Finland, http://www.voyantic.com/.